Journal of Ceramic Processing Research. Vol. 17, No. 11, pp. 1181~1187 (2016)

J O U R N A L O F
Ceramic Processing Research

Preparation of Al_2O_3-ZrO_2 composite powder by co-precipitation method in an alcohol-water solution and its sintering behavior

Jilin Hu*, Xiuying Tian, Chuanyue Hu, Yige Luo, Hongxia Peng and Jinqiu Luo

Hunan Provincial Key Laboratory of Fine Ceramics and Powder Materials, School of Materials and Environmental Engineering, Hunan University of Humanities, Science and Technology, Loudi 417000, China

Different types of aluminum sources (such as Al_2O_3 and $Al(OH)_3$) were used to prepare an Al_2O_3-ZrO_2 composite powder in an alcohol-water system, in which $ZrOCl_2 \cdot 8H_2O$ and NH_4HCO_3 were used as starting material and precipitant, respectively. This study explores the effects of different types of aluminum sources and heat treatment on the preparation of Al_2O_3-ZrO_2 composite powder. The sintering property of the Al_2O_3-ZrO_2 composite powder prepared from different types of aluminum sources was also investigated. Results indicate that Al_2O_3-ZrO_2 composite powder prepared from $Al(OH)_3$-containing precursors after calcination at 600 °C possesses a relatively uniform spherical structure, with particle size ranging from 50 nm to 100 nm. As the calcination temperature increases, the particle size of powder prepared using precursors that contain $Al(OH)_3$ increases and the micro appearance of the particles gradually shifts from a mainly spherical structure to a diversified structure, which can be spherical, sheet-like or rod-like. The Al_2O_3-ZrO_2 composite powder prepared from $Al(OH)_3$-containing precursors exhibits satisfactory sintering property. The relative density of the sintered sample reaches 98.5%, and the Rockwell hardness reaches 85.5 HRA after sintering of the composite powder at 1550 °C for 2 hrs.

Key words: Alumina-zirconia, Composite powder, Preparation, Alcohol-water system, Sintering behavior.

Introduction

High strength, hardness, and elasticity modulus, as well as heat resistance, chemical stability, electrical insulating property, and relative low production cost make Al_2O_3 ceramics an attractive structural and functional material for various applications [1-3]. However, the fracture toughness of Al_2O_3 ceramics is relatively low (usually 3 $MPa \cdot m^{1/2}$), thereby severely restricting the application and development of the material. In recent years, addition of second-phase particles to enhance the toughness of Al_2O_3 has gained increasing attention. The introduction of ZrO_2 into Al_2O_3 is an effective method used to improve the fracture toughness and strength of Al_2O_3 [4, 5]. The content and particle size of t-ZrO_2 significantly affect the fracture toughness of the resulting material [6]. High-quality composite powder can be used to prepare high-performance multi-phase ceramics. Consequently, the key step in the production of high-performance multi-phase ceramics is the preparation of the Al_2O_3-ZrO_2 composite powder, which features fine particle size, narrow and even particle size distribution, and tetragonal phase at ambient temperature.

Mechanical mixing is a simple and commonly used method to prepare composite powder. However, this method cannot guarantee the uniform dispersion of multiple components in the powder. Moreover, mechanical mixing may inhibit the toughening phase from playing an effective function and impair the mechanical property of the material [7]. As such, scholars have developed various techniques to prepare Al_2O_3-ZrO_2 composite powder, including sol-gel method [8], co-precipitation [9], hydrothermal method [10], chemical vapor deposition [11], self-propagating combustion [12], and other chemical synthesis methods. Traditional liquid-phase co-precipitation is used in aqueous solution. Nanopowder prepared using this method presents limitations, such as difficulty in controlling particle size and distribution, as well as the agglomeration tendency of the particles. Introduction of alcohol-water solution through liquid-phase co-precipitation synthesis can not only control particle size but also improve particle dispersion [13-16]. The preparation of Al_2O_3-ZrO_2 composite powder by using alcohol-water system has been rarely reported.

In this study, Al_2O_3-ZrO_2 (3 mol%Y_2O_3, 3Y) composite powder was prepared in alcohol-water solution. The effects of different types of aluminum sources and reaction temperature on phase composition, particle distribution, and micro appearance and sintering behavior of Al_2O_3-ZrO_2 (3Y) composite powder were investigated.

Experimental Procedure

The mole ratios of Al_2O_3 to t-ZrO_2 and Y_2O_3 to t-

*Corresponding author:
Tel : +86-738-8325065
Fax: +86-738-8325304
E-mail: hujilin@126.com

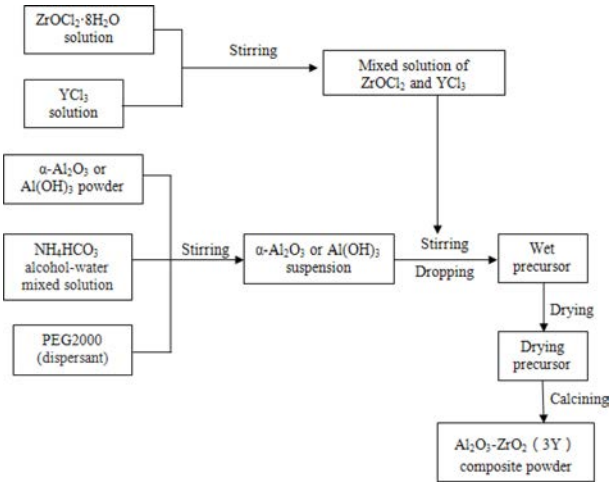

Fig. 1. The preparation process of the Al_2O_3-ZrO_2 (3Y) composite powder.

Table 1. The composition of Al_2O_3-ZrO_2 (3Y) sintered bodies.

Sample	Al_2O_3-ZrO_2(3Y) powders used	Al_2O_3-ZrO_2 (3Y)	TiO_2	CeO_2	La_2O_3
AZ1	Prepared from $Al(OH)_3$-containing precursors	94	3.0	1.5	1.5
AZ2	Prepared from Al_2O_3-containing precursors	94	3.0	1.5	1.5
AZ3	Commercially obtained	94	3.0	1.5	1.5

ZrO_2 are 4 : 1 and 3 : 97, respectively. In brief, 2 mol/L NH_4HCO_3 alcohol-water solution (the volume ratio of alcohol to water is 4 : 1) was prepared. The NH_4HCO_3 solution was added with a certain amount of α-Al_2O_3 or $Al(OH)_3$ powder and 1.5 wt.% dispersing agent (PEG2000) and churned for 1 h to dilute the suspension. Subsequently, 0.5 mol/L $ZrOCl_2·8H_2O$ solution was prepared. A certain amount of Y_2O_3 was added to hydrochloric acid to prepare the YCl_3 solution. The YCl_3 solution and $ZrOCl_2·8H_2O$ solution were completely mixed, and the mixed solution was slowly added to the α-Al_2O_3 or $Al(OH)_3$ suspension at a rate of 5 mL/min. The mixture was then churned in an agitator for 2 hrs. Absolute ethyl alcohol was used as titrant to separate ZrO_2 precursors from the solution during slow titration. The hybrid precursors were washed with water and alcohol for several times and then dried to obtain Al_2O_3-ZrO_2 (3Y) precursor precipitates. The precursors were ground with agate mortar and calcined at different temperature for 1 hr to obtain Al_2O_3-ZrO_2 (3Y) composite powder. The preparation process of Al_2O_3-ZrO_2 (3Y) composite powder is shown in Fig. 1.

Al_2O_3-ZrO_2 (3Y) composite powder prepared using an alcohol-water solution was mixed with a sintering aid in a mass ratio of 94 : 6. Al_2O_3 and ZrO_2 (3Y) were commercially obtained and mechanically mixed. The sintering properties of these materials were also compared. The composition of the sample is shown in Table 1. All raw materials were weighed separately, milled in a planetary ball mill through wet method for 2 hrs, and dried in an oven at 100 °C. An appropriate amount of 6 wt.% polyvinyl alcohol solution was used as binding agent and added to the dried powder. After complete mixing, the mixture was cured for 12 hrs, granulated using 40-mesh sieve, and compressed at 100 MPa into a disk-like billet. The pellets were sintered at 1550 °C for 2 hrs. After rough grinding, fine grinding, and polishing, the volume density of the sintered body was measured using Archimedes method. The hardness of the sintered body was assessed using a HRS-150 Rockwell hardometer.

The DTA-50 simultaneous thermal analyzer was utilized to assess the variations in the dried hybrid precursor powder in air as the temperature increased at a rate of 10 °C/min. X-ray diffraction (XRD, AL-Y3000, China) was used to analyze the phase composition of powder samples treated at different temperatures. Nicolet iS50 Fourier transform infrared spectrometer (FT-IR) was employed to qualitatively determine the chemical composition and molecular structure of the hybrid precursor. An Easysizer20 laser particle size analyzer was applied to determine the size and distribution of powder samples sintered at different temperature. Scanning electron microscopy (SEM, Nova Nano 230) was used to analyze the particle appearance of powder samples and the micro-structure of the sintered body.

Results and Discussion

Thermal decomposition behavior of precursors

Fig. 2 shows the TG-DTA)curve of $Al(OH)_3$-containing precursors. Significant mass losses are found in four sections in the TG curve when the temperature is below 550 °C. The first, second, third, and fourth mass losses occur when the temperature are below 220 °C, 220 °C-260 °C, 260°C-320 °C, and higher than 320 °C, respectively. At ambient temperature to 220 °C, a relatively wide, weak endothermic peak is found at 85 °C in the DTA curve; this finding could be due to the release of the absorbed water from the precursors, resulting in 1.73% mass loss. At 220 °C-260 °C, a weak endothermic peak appears at 253 °C in the DTA curve, and the discharge of crystallization water from the precursors leads to 2.96% mass loss. At 260 °C-320 °C, a sharp endothermic peak is found at 315 °C in the DTA curve; basic carbonates decompose into oxide, CO_2, NH_3, and structural water, which volatilize and lead to a relatively high mass loss of 19.61% [17]. At 320 °C-550 °C, several weak exothermic peaks are found in the DTA curve because of the decomposition of several organic impurities and the crystal structure transition of t-ZrO_2 [18, 19]. Fig. 3 shows the TG-DTA curve of α-Al_2O_3-containing precursors. A relatively high mass loss (4.29%) is observed in the TG curve; low mass loss is detected at temperatures exceeding

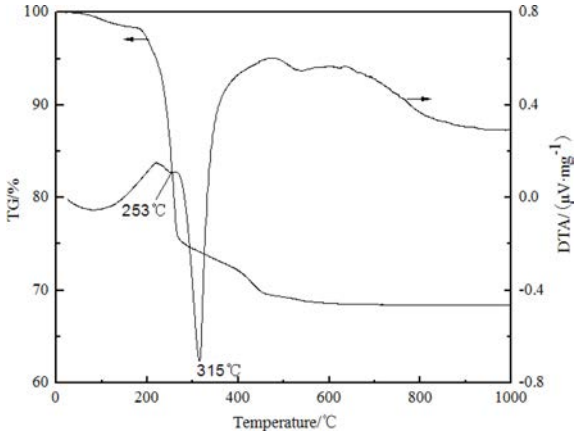

Fig. 2. The TG-DTA curve of $Al(OH)_3$-containing precursors.

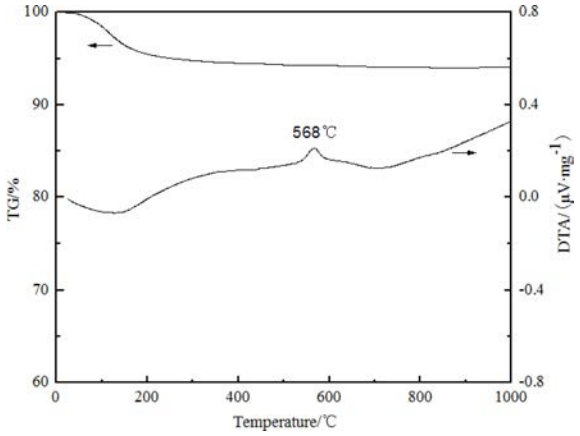

Fig. 3. The TG-DTA curve of α-Al_2O_3-containing precursors.

220 ºC, and a small mass loss of 1.66% is found at 220 ºC to 1000 ºC. In the DTA curve, a relatively wide weak endothermic peak is found at about 85 ºC, which could be due to the release in absorbed water from the precursors. An apparent exothermic peak appears at 568 ºC in the DTA curve and may be caused by the crystal structure transition of t-ZrO_2 [18].

Phase composition analysis

Fig. 4 shows the XRD spectrum of $Al(OH)_3$-containing precursors treated at different temperature. The precursors mainly exhibited the $Al(OH)_3$ diffraction peak but not the diffraction peak related to zirconium compound. Hence, the hybrid precursors mainly exist as a mixture of amorphous zirconium compound and crystalline $Al(OH)_3$. At treatment temperature exceeding 600 ºC, the diffraction peak of $Al(OH)_3$ disappears, whereas the diffraction peak of Al_2O_3 is not found in the spectrum; as such, the material remains amorphous. Moreover, an evident diffraction peak of tetragonal-phase ZrO_2 (t-ZrO_2) is found in the spectrum, implying that the zirconium compound already decomposed into ZrO_2 at this temperature. With increasing treatment temperature, the diffraction peak intensity of t-ZrO_2 in the spectrum

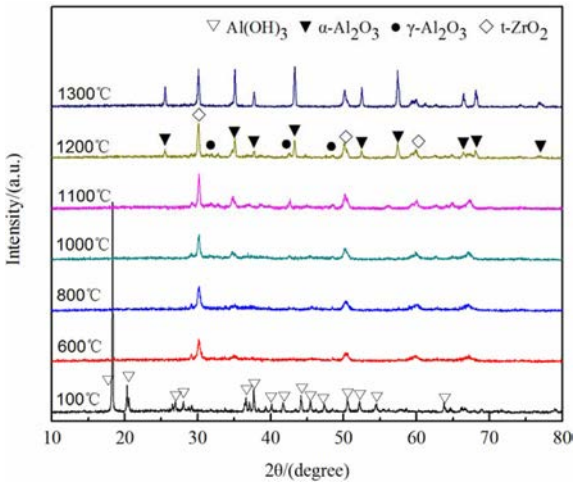

Fig. 4. The XRD spectrum of $Al(OH)_3$-containing precursors treated at different temperatures.

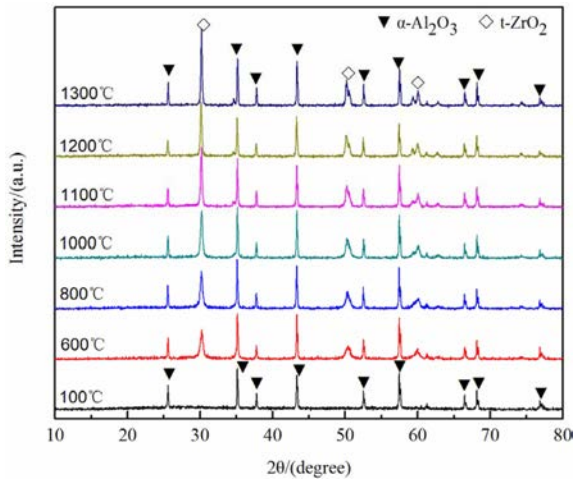

Fig. 5. The XRD spectrum of Al_2O_3-containing precursors treated at different temperatures.

also increases. At 1100 ºC, the diffraction peak of γ-Al_2O_3 is found in the spectrum and that of t-ZrO_2 is sharp. However, the diffraction peak of α-Al_2O_3 is not found in the spectrum, indicating that α-Al_2O_3 is not generated at this temperature. As the treatment temperature is further increased to 1200 ºC, a strong diffraction peak of α-Al_2O_3 is found in the spectrum, but the intensity of γ-Al_2O_3 diffraction peak decreases; as such, more α-Al_2O_3 principal crystallization phases are generated. At 1300 ºC, the diffraction peaks of α-Al_2O_3 and t-ZrO_2 are mainly found in the spectrum, and those of other crystalline phases are not found. In general, the crystalline phases of precursors containing Al_2O_3 may change upon calcination, that is, amorphous $Al_2O_3 \rightarrow \gamma$-$Al_2O_3 \rightarrow \theta$-$Al_2O_3 \rightarrow \alpha$-$Al_2O_3$. The phase of the pure ZrO_2-containing precursors may vary because of the mechanism of amorphous ZrO_2 t-ZrO_2 m-ZrO_2 [20, 21]. In this study, α-Al_2O_3 and t-ZrO_2 are the major products, and virtually no other interphase products are generated when the Al_2O_3-ZrO_2 composite

powder is calcined at different temperature and, with NH_4HCO_3 as the precipitant. On the one hand, Al_2O_3 powder is evenly dispersed around ZrO_2 powder particles when the composite powder contains a small amount of ZrO_2, leading to decreased ZrO_2 powder particles and imposing compressive stress on ZrO_2; consequently, phase transition from t-ZrO_2 to m-ZrO_2 is inhibited, and t-ZrO_2 is retained in the composite system. On the other hand, yttrium compound precursors in the composite powder can decompose into Y_2O_3 particles because the treatment temperature increases. Y_2O_3 particles combine with ZrO_2 to form a solid solution at high temperature [22], leading to high-temperature stability of t-ZrO_2 at ambient temperature. Fig. 5 presents the XRD spectrum of Al_2O_3-containing precursors at different treatment temperature. The diffraction peak of α-Al_2O_3 mainly exists in the spectrum of the precursors, and the zirconium compound is mainly amorphous. At 600 ºC, an apparent t-ZrO_2 diffraction peak appears in the spectrum in addition to the α-Al_2O_3 diffraction peak. As the treatment temperature increases, the XRD spectrum does not significantly change. Only the diffraction peak of the principal crystalline phase of t-ZrO_2 becomes sharper, indicating the high crystallization degree of the composite powder.

Analysis of precursor structure

Fig. 6 shows the FT-IR spectrum of $Al(OH)_3$-containing precursors. Absorption bands of the precursors are found at 730, 1016, and 1320-1530 cm^{-1}, which are the characteristic peaks of CO_3^{2-}. The absorption band appears at around 3437 cm^{-1} because of the stretching vibration of O-H radicals in the absorbed water. The absorption band at 3619 cm^{-1} is due to the existence of OH^-. The absorption band at 3360 and 3520 cm^{-1} is mainly attributed to the existence of crystallization water in the system. The absorption band at 968 cm^{-1} is caused by the presence of several C-C bonds in PEG-2000. Based on the XRD analysis and previous results [18], the reaction between $ZrOCl_2$ in the precursors and NH_4HCO_3 can be completed through two steps: first, both react to generate $Zr(OH)_4$, which subsequently reacts to generate water-soluble $(NH_4)_3ZrOH(CO_3)_3\cdot 2H_2O$. If the reaction system contains a certain amount of alcohol, $(NH_4)_3ZrOH(CO_3)_3\cdot 2H_2O$ could be precipitated from the solution. The reaction process is given below:

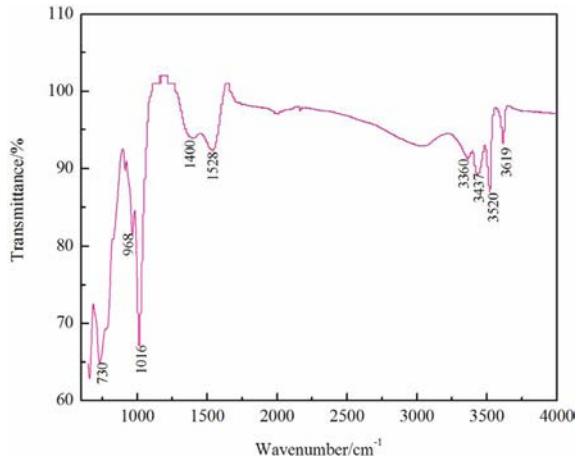

Fig. 6. The FT-IR spectrum of $Al(OH)_3$-containing precursors.

$$2NH_4HCO_3 + ZrOCl_2\cdot 9H_2O = Zr(OH)_4 + 2NH_4Cl + 2CO_2 + 8H_2O \quad (1)$$

$$3NH_4HCO_3 + Zr(OH)_4 = (NH_4)_3ZrOH(CO_3)_3\cdot 2H_2O \quad (2)$$

Analysis of particle size distribution

A laser particle size analyzer was employed to detect the particle size of the two types of Al_2O_3-ZrO_2 (3Y) composite powder obtained after heat treatment at different temperature. The results are displayed in Tables 2 and 3. Comparison of the median particle size of the powder samples between Tables 2 and 3 shows that the median particle size D_{50} of $Al(OH)_3$-containing precursors after calcination at different temperature is smaller than that of the powder prepared from Al_2O_3-containing precursors. As shown in Table 2, the median particle size of the sample is D_{50} = 0.45 μm at 600 ºC. The median particle size of the powder sample increases as the calcination temperature increases and reaches D_{50} = 0.84 μm at 1000 ºC. When the calcination temperature is further increased to 1300 ºC, the median particle size of the sample increases to D_{50} = 1.85 μm. As shown in Table 3, the median particle size of the sample is D_{50} = 4.06 μm at 600 ºC. The particle size of the powder sample shows an increasing trend with the increase in calcination temperature. The median particle size of the powder sample reaches D_{50} = 5.84

Table 2. The particle size of $Al(OH)_3$-containing precursors treated at different temperatures. [μm]

NO.	Temperatures /ºC	D_{10}	D_{25}	D_{50}	D_{75}	D_{90}
1	600	0.23	0.32	0.45	0.52	0.73
2	800	0.32	0.43	0.51	0.58	0.79
3	1000	0.40	0.62	0.84	1.28	2.33
4	1100	0.46	0.88	1.35	1.85	3.27
5	1200	0.53	0.95	1.59	2.12	4.18
6	1300	0.56	1.03	1.85	2.57	5.08

Table 3. The particle size of Al_2O_3-containing precursors treated at different temperatures. [μm]

NO.	Temperatures / °C	D_{10}	D_{25}	D_{50}	D_{75}	D_{90}
1	600	0.60	1.85	4.06	7.64	14.29
2	800	0.72	2.23	4.58	8.16	15.75
3	1000	0.92	2.77	5.84	10.96	16.42
4	1100	0.62	2.48	5.87	11.53	16.70
5	1200	0.61	2.72	6.13	11.36	16.65
6	1300	0.68	2.85	6.45	11.56	16.87

and 6.45 μm at 1000 °C and 1300 °C, respectively.

Analysis of micro appearance

Fig. 7 shows the SEM picture of Al_2O_3-ZrO_2 (3Y) composite powder samples after α-Al_2O_3-containing precursors are calcined at 600 °C and $Al(OH)_3$-containing precursors are calcined at different temperature. Comparison of Figs. 7(a) and 7(b) shows that the powder sample prepared from α-Al_2O_3-containing precursors possess a similar structure to colloids at calcination temperature of 600 °C; that is, 100-200 nm fine particles aggregate to form an encapsulated structure. However, powder prepared from $Al(OH)_3$-containing precursors presents a uniform spherical structure and even particle size distribution, mostly within 50-100 nm. This finding indicates that hybrid precursors prepared in the alcohol-water solution can be calcined at 600 °C to produce ultra-fine Al_2O_3-ZrO_2 (3Y) composite powder with good dispersion and uniform particle size. When a certain amount of alcohol is present in the water solution, the dielectric permittivity

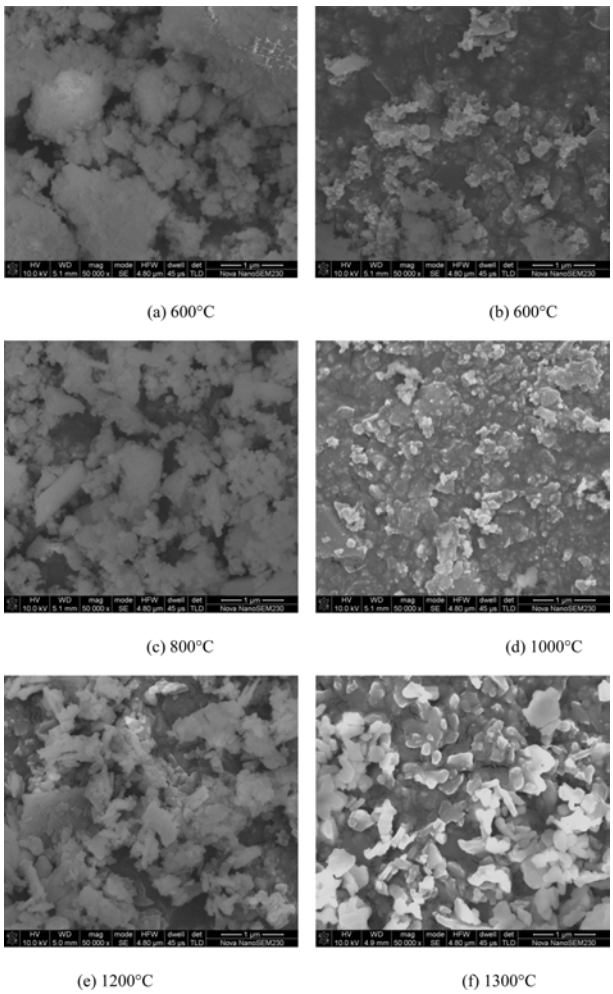

Fig. 7. The SEM picture of Al_2O_3-ZrO_2 (3Y) composite powder samples after α-Al_2O_3-containing precursors are calcined at 600 °C and $Al(OH)_3$-containing precursors are calcined at different temperatures: (a) α-Al_2O_3-containing precursors and (b)~(f) $Al(OH)_3$-containing precursors.

of alcohol is lower than that of water; this phenomenon decreases the dielectric permittivity of the solution and the solubility of the synthetic product to a certain extent, thereby facilitating the generation of fine particles. Hydroxide radicals are also present in alcohol, eliciting steric hindrance effect; this effect could restrict particle aggregation and confer protection for fine particles [14, 23]. As such, when the volume ratio of alcohol to water is appropriate in the reaction system, numerous fine nuclei could be formed among reactants, thus causing primary particles to be covered by alcohol molecules, preventing the particles from aggregation, and leading to dispersion of the particles. As calcination temperature increases, the particle size of the powder gradually increases. When the calcination temperature is increased to 800 °C, powder prepared from $Al(OH)_3$-containing precursors exhibits a similar structure to the colloidal structure shown in Fig. 7, and particle size increases. When the calcination temperature increased to 1000 °C, a slight sintering phenomenon is found in the micro structure of the powder sample. With continuous increase in calcination temperature, the appearance of the powder sample changes. Powder particles are mainly spherical at low calcination temperature. At high temperature, the particles present diverse structures, including spherical, rod-like, and sheet-like, and particle size increases. As the sintering phenomenon among the powder particles intensifies, large particles are formed, indicating the high sintering activity of the Al_2O_3-ZrO_2 (3Y) powder sample.

Sintering behavior of composite powder

Table 4 shows the volume density and Rockwell hardness of the sintered bodies obtained after the three types of Al_2O_3-ZrO_2 (3Y) composite powders are sintered at 1550 °C for 2 hrs. The volume density and Rockwell hardness of the samples obtained after the composite powder prepared in the alcohol-water system is sintered at 1550 °C are higher than those of the sintered sample prepared from the mixture of different commercially purchased powders. The relative density and Rockwell hardness of AZ1 sintered sample reach 98.5% and 85.5 HRA, respectively. The sintering property of AZ3 sintered sample is relatively poor, and the relative density and Rockwell hardness are 95.7% and 77.8 HRA, respectively.

Fig. 8 shows the micro structure of samples obtained after three types of Al_2O_3-ZrO_2 (3Y) composite powders are sintered at 1550 °C for 2 hrs. As shown in Fig. 8a, the microstructure of the sintered sample is relatively dense and uniform; thus, the sample presents relatively high density and Rockwell hardness. Microstructures with relatively low density are formed in the AZ2 sample (Fig. 8(b)); hence, several structures are loose and porous, few large particles exist in the sample, and particle uniformity is lower than that in AZ1 sample. In Fig. 8(c), more particles are found on the surface of the

Table 4. The relative density and Rockwell hardness of the sintered bodies.

Sample	Al_2O_3-ZrO_2(3Y) powders used	Relative density (%)	Hardness (HRA)
AZ1	Prepared from $Al(OH)_3$-containing precursors	98.5	85.5
AZ2	Prepared from Al_2O_3-containing precursors	97.4	82.4
AZ3	commercially obtained	95.7	77.8

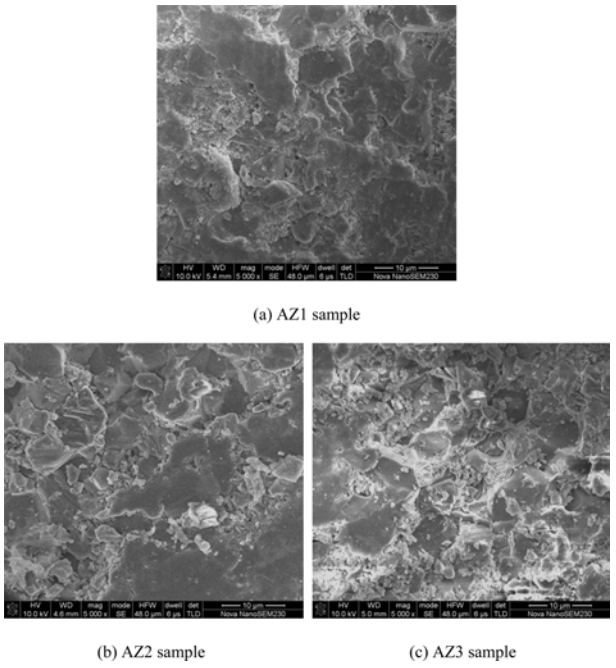

(a) AZ1 sample

(b) AZ2 sample (c) AZ3 sample

Fig. 8. SEM images of Al_2O_3-ZrO_2 (3Y) composite powder sintered at 1550 °C for 2 hrs.

sintered sample; these particles are large and exhibit poor uniformity, thereby adversely influencing the density and mechanical property of the Al_2O_3-ZrO_2 (3Y) sintered sample. The microstructure analysis result of the three types of Al_2O_3-ZrO_2 (3Y) sintered samples is consistent with the analysis result of the relative density and Rockwell hardness. Thus, the powder sample obtained after $Al(OH)_3$-containing precursors are calcined at 600 °C exhibits good sintering property.

Conclusions

Calcination temperature significantly affects the phase composition of Al_2O_3-ZrO_2 (3Y) composite powder. In the precursors, the zirconium compound is mainly amorphous. When the calcination temperature is 600 °C, a strong t-ZrO_2 diffraction peak appears in the powder, and the $Al(OH)_3$ diffraction peak in the precursors disappears. The product Al_2O_3 obtained by the decomposition of $Al(OH)_3$ remains amorphous. When the calcination temperature increases to 1200 °C, strong α-Al_2O_3 and t-ZrO_2 diffraction peaks are found in the XRD spectrum of the powder sample.

When the calcination temperature is 600 °C, the powder sample prepared from α-Al_2O_3-containing precursors possess a similar structure to that of colloid; that is, numerous 100-200 nm fine particles aggregate to form an encapsulated structure. Basically, the powder sample prepared from $Al(OH)_3$-containing precursors possesses a uniform spherical structure and even particle size distribution, mostly within the range of 50-100 nm. The powder particle size increases with the increase in calcination temperature. Moreover, the micro-appearance of powder is mainly spherical at first; as the temperature rises, the particle shape tends to be diversified, including spherical, rod-like, and sheet-like. The sintering phenomenon among the powder particles is also intensified.

The volume density and Rockwell hardness of samples obtained after sintering the Al_2O_3-ZrO_2 (3Y) composite powder at 1550 °C in the alcohol-water system are higher than those of the sintered sample prepared from the mixture of different powders bought from the market. Among the three sintering samples, the AZ1 sample exhibits high density and uniform microstructure, as well as the highest relative density and Rockwell hardness among samples, reaching 98.5% and 85.5 HRA, respectively.

Acknowledgments

This work is supported by the Natural Science Foundation of Hunan Province, China (Grant No. 2016JJ6047), the Planned Science and Technology Program of Hunan Province, China (Grant No. 2016TP1028) and the ChanXueYan Special Funds of the Hunan University of Humanities, Science and Technology, China (Grant No. 2014CXY03).

References

1. J.L. Yang, X.X. Xu, J.M. Wu, X.H. Wang, Z.G. Su and C.H. Li, J. Eur. Ceram. Soc. 35 (2015) 2593-2598.
2. C.L. Zhou, B.X. Jiang, J.T. Fan, X.J. Mao, L.J. Pan, Y.G. Jiang, L. Zhang and Y.Z. Fang, Ceram. Int. 42 (2016) 1648-1652.
3. H.T. Li, Q.L. Liao, Y.Y. Dai, F. Wang, H.Y. Wang and X.B. Li, Mater. Res. Bull. 76 (2016) 311-316.
4. A. Safinajafabadi, R. Sarraf-Mamoory and Z. Karimi, Mater. Res. Bull. 47 (2012) 4210-4215.
5. D.G. Liu, Y. Gao, J.L. Liu, F.Z. Liu, K. Li, H.J. Su, Y.G. Wang and L.N. An, Scripta Mater. 114 (2016) 108-111.
6. A. Rittidech and T. Tunkasiri, Ceram. Int. 38 (2012) S125-S129.
7. J. Zárate, H. Juárez, M.E. Contreras and R. Pérez, Powder Technol. 159 (2005) 135-141.
8. B.T. Lee, J.K. Han and F. Saito, Mater. Lett. 59 (2005) 355-360.
9. L.F. Xu, P. Li, X.A. Xi, A.Z Shui, W.L. Zhu and W.B. Dai, J. Alloys Compd. 656 (2016) 798-804.
10. M. Herrmann, B. Seipel, J. Schilm, K.G. Nickel, G. Michael

and A. Krell, J. Eur. Ceram. Soc. 25 (2005) 1805-1812.
11. A. Ito, Y. You, T. Ichikawa, K. Tsuda and T. Goto, J. Eur. Ceram. Soc. 34 (2014) 155-159.
12. S. Biamino, E.P. Ambrosio, D. Manfredi, P. Fino and C. Badini, J. Ceram. Process Res. 12 (2011) 207-211.
13. S.H. Tong, T.C. Lu and W. Guo, Mater. Lett. 61 (2007) 4287-4289.
14. C.H. Zhang, X. Huang, Y.S. Yin, J.H. Dai and Z.B. Zhu, Ceram. Int., 35 (2009) 2979-2982.
15. M.H. Wang, X.Y. Ma, W. Jiang and F. Zhou, Mater. Lett. 121 (2014) 149-151.
16. A.L. Bai, H. Song, G.Y. He, Q.S. Li, C. Yang, L.M. Tang and Y.M. Yu, Ceram. Int., 42 (2016) 7583-7592.
17. G.S.A.M. Theunissen, J.S. Bouma, A.J.A. Winnubst and A.J. Burggraaf, J. Mater. Sci. 27 (1992) 4429-4438.
18. J.N. Tang, X.H. Jin and L. Gao, J. Inorg. Mater. 18 (2003) 1367-1371.
19. D. Sarkar, D. Mohapatra, S. Ray, S. Bhattacharyya, S. Adak and N. Mitra, Ceram. Int. 33 (2007) 1275-1282.
20. K. Yamakata, K. Hirota and O. Yamaguchi, J. Am. Ceram. Soc. 77 (1994) 2207-2208.
21. M. Yoshimura, S.T. Oh, M. Sando and K. Niihara, J. Alloys Compd. 290 (1999) 284-289.
22. H.L. Chu, W.S. Hwang, J.K. Du, K.K. Chen and M.C. Wang, Ceram. Int. 42 (2016) 10251-10258.
23. J.Q. Wang, X. Li, S.P. Li and H. Zhong, Acta Chim. Sinica 69 (2011) 137-144.